



Soil Moisture Estimation by GNSS-IR from Active Stations: Case Study – RBMC/IBGE, UFPR Station

Estimativa da Umidade do Solo por GNSS-IR a partir de Estações Ativas: Estudo de Caso – RBMC/IBGE, Estação UFPR

Jorge Felipe Euriques¹ , Luis Augusto Koenig Veiga² , Wagner Carrupt Machado³ ,
Claudia Pereira Krueger²  & Felipe Geremia Nievinski⁴ 

¹Universidade Federal Rural do Rio de Janeiro, Instituto de Tecnologia, Departamento de Engenharia, Rio de Janeiro, RJ, Brasil

²Universidade Federal do Paraná, Setor de Ciências da Terra, Departamento de Geomática, Curitiba, PR, Brasil

³Universidade Federal de Uberlândia, Instituto de Geografia, Geociências e Saúde Coletiva, Uberlândia, MG, Brasil

⁴Universidade Federal do Rio Grande do Sul, Instituto de Geociências, Departamento de Geodésia, Porto Alegre, RS, Brasil

E-mails: jorge.euriques@ufrj.br; kngveiga@ufpr.br; wagnercarrupt@ufu.br; [cpkrueger@ufpr.br](mailto:cpkruieger@ufpr.br); felipe.nievinski@ufrgs.br

Abstract

The Earth is a dynamic planet subject to numerous natural phenomena and processes that human activities have intensified. Monitoring variables associated with these phenomena is essential. Soil moisture, for example, plays a crucial role in climate systems, agriculture, and the hydrological cycle. The Global Navigation Satellite Systems (GNSS) is one of the Geodesy tools used for monitoring the Earth, through which the GNSS Interferometric Reflectometry (GNSS-IR) technique can be employed to estimate soil moisture. In this study, the UFPR station, part of the Brazilian Continuous Monitoring Network of GNSS Systems (RBMC) was selected for investigation. A Python script was developed to automate the preparation of GNSS data from any RBMC station. Different processing configurations of a reflectometric algorithm were evaluated, resulting in a set of time series of soil moisture for 2022. Results indicate that configurations adapted to the station's local conditions contribute to the enhancement of the results. The best signal among the 24 evaluated was the precise signal from the L2 frequency of GLONASS (RS2P). Peaks in precipitation were aligned with peaks in soil moisture, with soil moisture ranging from 0 to 0.35 m³/m³. The results support the development of a methodology for monitoring soil moisture in the vicinity of GNSS-RBMC stations that meet GNSS-IR requirements, expanding the potential applications of this network.

Keywords: Interferometric reflectometry; Geodetic remote sensing; Hydrological cycle

Resumo

A Terra é um planeta dinâmico sujeito a inúmeros fenômenos e processos naturais que as atividades humanas têm intensificado. O monitoramento das variáveis associadas a estes fenômenos é essencial. A umidade do solo, por exemplo, desempenha um papel crucial nos sistemas climáticos, na agricultura e no ciclo hidrológico. O *Global Navigation Satellite System* (GNSS) é uma das ferramentas da Geodésia empregadas no monitoramento da Terra e, por meio da Refletometria Interferométrica GNSS (do inglês, *GNSS Interferometric Reflectometry* - GNSS-IR) possibilita estimar a umidade do solo. Neste estudo, a estação UFPR, integrada a Rede Brasileira de Monitoramento Contínuo dos Sistemas GNSS (RBMC), foi selecionada para uma investigação. Um script em Python foi desenvolvido para automatizar a preparação dos dados GNSS para GNSS-IR provenientes de qualquer estação da RBMC. Diferentes configurações de processamento de um algoritmo refletométrico foram avaliadas, resultando em um conjunto de séries temporais de umidade do solo para 2022. Os resultados indicaram que as configurações adaptadas às condições locais da estação contribuíram com o aprimoramento dos resultados. O melhor sinal, dentre os 24 avaliados, foi o sinal preciso pela onda portadora L2 do GLONASS (RS2P). Os picos de umidade do solo mostraram-se alinhados com os picos de precipitação, com níveis de umidade do solo variando de 0 a 0,35m³/m³. Os resultados apoiam o desenvolvimento de uma metodologia para o monitoramento de umidade do solo no entorno de estações GNSS-RBMC que atendem aos requisitos da GNSS-IR ampliando as aplicações potenciais desta rede.

Palavras-chave: Refletometria interferométrica GNSS; Sensoriamento remoto Geodésico; Ciclo hidrológico

1 Introduction

Earth is a dynamic planet susceptible to numerous processes. Changes in the Earth System are a natural consequence of these processes. However, due to human activities, the changes occurring over the last 150 years are incomparable to those that occurred previously (Simon et al. 2006). Population growth, combined with increasing exploitation of natural resources, has led to drastic changes on the planet, such as global warming, which affects the climate system and, consequently, Earth's dynamics. This scenario has resulted in a decrease in freshwater reserves and an increase in the occurrence of extreme phenomena (Awange & Kiema 2013). According to Plag and Pearlman (2009), sustainable development is crucial for achieving a stable future for the planet.

Monitoring processes related to the Earth System is one of the prerequisites for sustainable development (Paganini et al. 2018). These considerations are highlighted in the plan titled "Transforming Our World: The 2030 Agenda for Sustainable Development" (Agenda 2030), proposed by the United Nations in 2014 (Acharya & Lee 2019).

Soil moisture is the water content present in the vadose zone of the soil and is a quantity related to numerous hydrological, geophysical, and environmental phenomena of the Earth that manifest at different scales (Hillel 1998; Seneviratne et al. 2010). It plays an essential role in biogeochemical cycles, such as those of water and carbon, and is related to the energy flows between the Earth's physical surface and the atmosphere. Soil moisture quantification is critical for managing water resource management and has numerous applications, including weather forecasting; delineation of flood areas and groundwater recharge; geotechnics; engineering works; and agriculture (Robinson et al. 2008; Entekhabi et al. 2010; Seneviratne et al. 2010; Ochsner et al. 2013; Edokossi et al. 2020; Zhang et al. 2021; Wu et al. 2021).

Contact probes and Remote Sensing are the most common methods for estimating soil moisture (Babaecian et al. 2019). In the former case, measurements are point-based and may not represent an area of interest. On the other hand, Remote Sensing offers global coverage, but with generalized information due to the spatial resolution of approximately 100 m for radars and 10 km for radiometers (Edokossi et al. 2020; Vey et al. 2016).

According to Plag and Pearlman (2009), geodesy provides fundamental information on changes in the Earth's shape, gravitational field, and rotation, referred to as the pillars of geodesy. The quantities associated with

these pillars are directly related to mass transport and the dynamics of the Earth System.

The Global Navigation Satellite Systems (GNSS) is one of the four space techniques in geodesy (Altamimi et al. 2016). GNSS encompasses various satellite positioning systems, originally developed for determining position, navigation, and timing (Seeber, 2003). However, the signals transmitted by GNSS satellites have been explored for other purposes, such as Remote Sensing through the technique known as GNSS Reflectometry (GNSS-R), which involves the joint reception of direct signals intended for positioning and indirect signals resulting from reflections over surfaces surrounding the GNSS antenna, giving rise to the so-called multipath effect (Zavorotny & Voronovich 2000; Georgiadou & Kleusberg 1988; Teunissen & Montenbruck 2017; Leick 1995).

GNSS Reflectometry conducted from conventional GNSS stations focused on positioning and exploiting the multipath effect, is called GNSS Interferometric Reflectometry (GNSS-IR). Indirect signals, therefore, those that do not originate from a direct path between the satellite and the GNSS antenna, affect accurate positioning but enable GNSS-IR. These indirect signals are recorded by the antenna with a time delay due to the additional path compared to the direct signal. When interacting with reflecting surfaces, these signals have their characteristics (amplitude, phase, frequency, and polarization) changed based on the composition, dielectric properties, and roughness of the surface. These changes are also related to the angle of incidence of the signal and the height of the GNSS antenna relative to the reflecting surface (Larson & Nievinski 2013; Roussel et al. 2015; Zavorotny et al. 2014). By combining information from direct and reflected signals, properties of the reflecting surface, and characteristics of the GNSS equipment, it is possible to estimate attributes of these surfaces, such as soil moisture, vegetation growth, and water levels (Jin et al. 2014).

Estimating soil moisture is one of the applications in which GNSS-IR has been successfully employed (Larson et al. 2008a; Rodriguez-Alvarez et al. 2009; Larson et al. 2010; Chew et al. 2014; Arroyo et al. 2014; Tabibi et al. 2015; Roussel et al. 2016; Vey et al. 2016; Yan et al. 2018; Euriques, 2019; Yang et al. 2019; Zhang et al. 2021; Li et al. 2022; Wang et al. 2022; Wei et al. 2023). Two of the main advantages of GNSS-IR over conventional soil moisture estimation methods are an intermediate coverage area of about 50 meters for an antenna at a height of 2 meters; and the use of the well-established GNSS infrastructure, which ensures appropriate temporal resolution (Tabibi et al. 2017; Euriques et al. 2021).

Although all GNSS observables are affected by multipath, the Signal-to-Noise Ratio (SNR) is the observable that best reveals this effect. SNR is invariant to common effects between direct and indirect paths that impact other observables, such as relative orbital errors; much of the atmospheric delays; and clock synchronization errors (Larson et al. 2010).

In the case of soil moisture, the desired metrics from SNR modeling are the phase parameters of the reflected signal. These values are converted into soil moisture through a calibration curve. A polynomial establishes the relationship between the interferometric phase parameters and the soil moisture values (Chew et al. 2014; Vey et al. 2016). The main limitations of this methodology are the imprecision of the theoretical coefficients of the calibration curve and factors related to the modeling of interferometric signals, such as the effects of topography and vegetation (Euriques et al. 2021; Zhang et al. 2017).

A reflectometric algorithm via SNR was developed in Matlab by Nievinski & Larson (2014a, 2014b, 2014c, 2014d) for snow altimetry; it was adapted for soil moisture estimation by Tabibi et al. (2015) and expanded for Multi-GNSS by Tabibi et al. (2017). Euriques (2019), used this algorithm to estimate soil moisture around a station installed at the National Institute for Space Research (In Portuguese, Instituto Nacional de Pesquisas Espaciais - INPE) in Cachoeira Paulista - SP, marking the first results of this application in Brazil. In this research, a correlation of 73% was obtained between the GNSS-IR estimates and a probe from the Cosmic-ray Soil Moisture Observing System, used for validation. Alternatively, the software Gnsrefl was made available to the scientific community; this is an open-source software developed in Python for GNSS-IR (Larson 2024). The Gnsrefl includes specific modules for various applications, including a module for estimating soil moisture.

The efficiency of the technique has been demonstrated by numerous international studies that reported a high correlation with conventional equipment. For example, Larson et al. (2008b) achieved an 85% correlation between GNSS-IR and moisture results from ten Time Domain Reflectometry (TDR) probes; Roussel et al. (2016) obtained correlations of up to 95% with capacitance probes; Yang et al. (2017) validated GNSS-R results using modeled values of soil permittivity, achieving correlations of up to 70%; in turn, Martín et al. (2020) validated GNSS-IR results with the gravimetric method, considered the most accurate method, obtaining correlations of up to 85%.

Every GNSS antenna is subject to receiving indirect signals and, consequently, to the multipath effect.

Thus, reflectometric determinations can be made from GNSS tracking aimed at positioning, without requiring modifications to the equipment or the antenna installation (Larson et al. 2010). This allows for the possibility of employing historical series, for example, from active GNSS stations, for reflectometric applications, enabling the enhancement of phenomenon modeling.

In this context, data from continuously operating GNSS stations, referred to as active stations, such as those in the Brazilian Continuous Monitoring Network of GNSS Systems (RBMC), maintained by the Brazilian Institute of Geography and Statistics (IBGE), can be used, expanding the range of applications for this network. However, not all stations are suitable for GNSS-IR, as certain assumptions are required (Nievinski et al. 2016). First, the location of the GNSS station must be considered. For soil moisture estimation, the area surrounding the antenna must be predominantly bare soil or low vegetation. Additionally, there must be unobstructed visibility to the ground in that area (Geremia-Nievinski; Hobiger 2019).

The scope of this research consisted of estimating soil moisture around a RBMC station by GNSS-IR, aiming to present methodological guidelines for automating the processing of SNR data via a reflectometric algorithm to enable soil moisture monitoring, thereby expanding the range of applications of the RBMC.

2 Data and Methodology

Figure 1 corresponds to the methodological flowchart of this research, which began with an evaluation of RBMC stations to select one for the study. Next, the SNR recorded in the station's RINEX files was analyzed using the RTKlib software and the GNSS Reflections tool (<https://gns-reflections.org/rzones>). An algorithm was developed in Python to enable the download, conversion, and standardization of GNSS data from the RBMC. A topographic survey was conducted to map the obstructions surrounding the station to establish processing configurations. Subsequently, the data were processed using the reflectometric algorithm developed by Nievinski and Larson, from which two signals that showed the best results were selected: one from the United States Global Positioning System (GPS) and another from the Russian system (GLONASS). Thus, two series of reflectometric phase data were obtained, and then converted to soil moisture series using the calibration curve, employing coefficients established in the literature. The results were compared with precipitation events recorded by an automatic station from the National Institute of Meteorology (In Portuguese, Instituto Nacional de Meteorologia INMET).

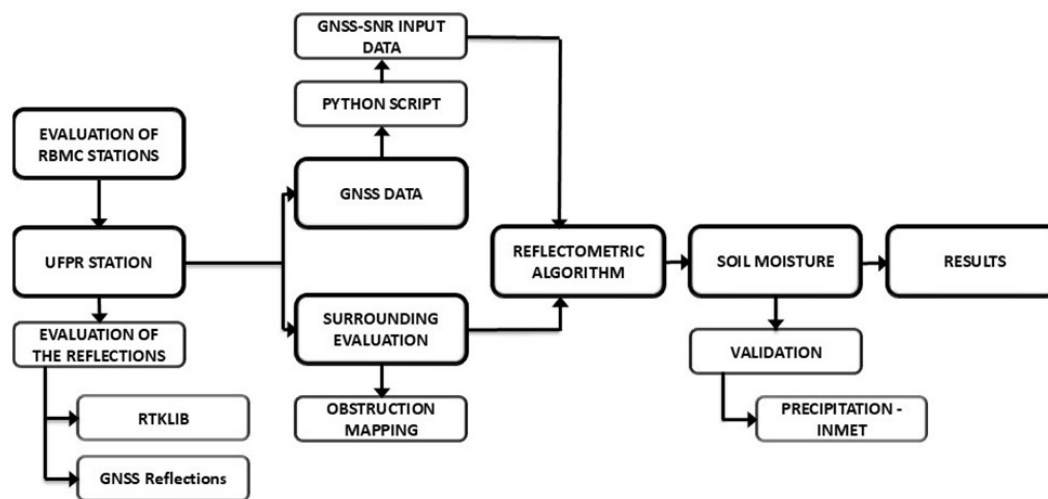


Figure 1 Flowchart of methodology.

2.1 Selection of Reference Station: UFPR-RBMC

The RBMC currently has 146 active GNSS stations distributed throughout the national territory (IBGE & RBMC 2024). However, not all stations are suitable for estimating soil moisture using GNSS-IR. This technique has assumptions, primarily related to the characteristics of the reflected signals.

One initial condition is the ground cover in the area of interest, also called the footprint, which should be predominantly exposed soil or low vegetation. This area refers to the surface reflecting the GNSS signals, which can be approximated by a set of ellipses known as Fresnel zones (Geremia-Nievinski & Hobiger 2019). This coverage varies for each station, as the dimensions of each ellipse depend on the height of the antenna, the elevation angle, and the wavelength of the signal. Another requirement is that there must be unobstructed visibility between the GNSS antenna and the ground so that the reflected signals are not affected by obstructions. In this sense, most stations are often not suitable for this application, as they are predominantly located in urban areas near buildings or on paved ground.

A preliminary selection of the stations was made by visually evaluating the surrounding composition using the station memorial provided by IBGE, Google Earth, and Street View. Table 1 lists some of the pre-selected stations and their classifications. After the visual assessment of the surrounding areas of the stations, the UFPR station, located in Curitiba-PR, was chosen. Although this station

was classified with a ‘moderate’ status in the visual evaluation presented in Table 1, due to the presence of some obstructions such as trees, buildings, metal structures, and mainly a wall, the UFPR station was selected based on the following considerations: 1) defining a methodology using a non-ideal station allows for easier replication in other stations; 2) one of the existing buildings in the area and the metal structures belong to an INMET station. The presence of a nearby INMET station is beneficial, as it allows for a more accurate comparison of the results with the meteorological variables observed by that station; 3) logistical advantages allowed for better control of factors affecting reflections, such as controlling the height of the grass; 4) due to the inclination of the orbital plane of global GNSS satellites, there is an absence of Fresnel zones in the southern direction for stations located in the Southern Hemisphere, and it is in this region that the surrounding buildings of the antenna are located.

The UFPR station (Figure 2) is located on the Polytechnic Center campus of the Federal University of Paraná. It began operations in 2007, replacing the old PARA station. The structure consists of a pillar with a height of 1.20 meters above the ground, equipped with a forced centering device and an extension. The antenna, a Zephyr 3 Geodetic model (TRM115000.00), has a height of 0.10 meters between the Antenna Reference Point (ARP) and the top of the pillar. The GNSS receiver of this station is a Trimble NETR9. The current antenna and receiver set were installed on April 4, 2018 (IBGE & RBMC 2024).

Table 1 Examples of analyzed RBMC stations. The strikethrough line (MSCG) refers to a deactivated station. The bolded line refers to the station under study in this research (UFPR).

Station	Location	% of ground visibility	Notes	Status
RSAL	Alegrete - RS	40	Parking	Bad
MSAQ	Aquidauana - MS	90	Bare Soil/fence	Good
SEAJ	São Cristóvão - SE	30	Large Trees/Buildings	Bad
ALAR	Arapiraca - AL	10	Buildings e sidewalk	Bad
SCAQ	Araquari - SC	70	Access roads and trees	Bad
MGBH	B. Horizonte - MG	0	Without ground visibility	Bad
MTCA	Cáceres - MT	90	Cropland/fence	Good
MSCG	C. Grande - MS	70	Inactive Station	Good
MSNV	Naviraí - MS	90	Cropland/fence	Good
SPBO	Botucatu - SP	40	Grassland/Buildings	Moderate
UFPR	Curitiba	70	Grassland/wall	Moderate
BOAV	Boa Vista - RR	80	Bare Soil/fence	Good

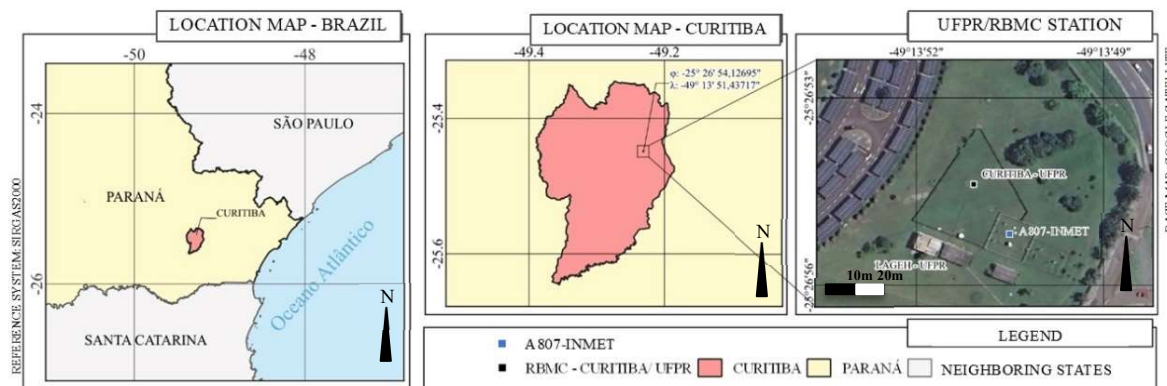


Figure 2 UFPR station location.

2.2 CURITIBA-A807 Meteorological Station

The INMET meteorological station, named CURITIBA-A807, is located about 30 meters from the GNSS station. This station is part of a network of automatic stations, consisting of a central memory unit connected to various sensors for measuring meteorological parameters such as atmospheric pressure, air temperature and relative humidity, precipitation, solar radiation, wind direction, and speed (INMET 2024). The data recorded by these sensors are integrated and automatically stored every hour and can be accessed through the INMET portal. Precipitation events, measured by a rain gauge at this station, were used for comparison with the GNSS-IR soil moisture estimates.

2.3 Evaluation of Reflected Signals

The behavior of reflected signals at the UFPR station was evaluated through visible oscillations in the SNR series. This step is performed by analyzing the oscillations present in the SNR time series, allowing for an estimation of whether the reflections are being affected by obstructions. Obstructions generate noise in the series and impair the pattern of these oscillations. The lower the satellite’s elevation angle, the greater the chance of being affected by obstructions around the antenna. Thus, well-defined oscillations near the satellite’s rise and set, coming from low elevation angles, indicate the intact reception of reflected signals for the considered azimuth. It is worth



noting that GNSS-IR exploits signals from satellites with elevation angles up to 30 degrees, with exceptions for studies addressing specific methodologies.

To perform this step, the RTKPLOT software from the RTKLIB package, version 2.4.2, was used, along with RINEX observation files (RINEX.o) and navigation files (RINEX.n) from the UFPR station for the first week of 2022, each of these files corresponding to 24 hours. This analysis could have been performed with just one day’s RINEX files; however, the consistency of the analysis was evaluated over seven days to refine the results. The SNR curves for each combination of satellite and modulation from the GPS and GLONASS systems were assessed.

Figure 3A refers to the skyplot, which shows the satellite (G15) trajectories during two passes over the antenna’s horizon during the evaluation period. The first pass occurred on the Western (W) portion of the GNSS station, following approximately the North (N) – South (S) direction. The second pass occurred on the Eastern (E) portion. In Figure 3B there is a southeast view of the station, where obstructions such as trees, metal structures, and buildings can be observed.

Subsequently, an evaluation was conducted using the GNSS-IR Reflection Zone Mapping tool (<http://gnss-reflections.org/>), which allows for preliminary analyses of the station directly related to GNSS-IR. Figure 4 presents the reflection surfaces of the signals (Fresnel zones), considering two scenarios. In the first scenario (Figure 4A), the coverage area was defined considering elevation angles between 5° (yellow) and 25° (cyan) with an interval of 5°. The higher the elevation angle, the smaller the semi-major axis of the ellipse. It can be noted that with this configuration, the reflection area encompasses direct obstructions to the reflected signals, such as solar panels (left side), a building, trees, and many metal structures from the meteorological station. In the second scenario (Figure 4B), a mask was applied in terms of elevation angles to consider elevation angles between 10 and 15 degrees (10° in yellow, and 20° in red). In this case, although there is a smaller area, it will be less susceptible to obstructions for the reflected signals, making it more suitable for the technique.

The results of this stage were combined with the obstruction mapping to define a filter in terms of azimuth and elevation so that signals from areas with significant obstructions could be disregarded in the processing stage.

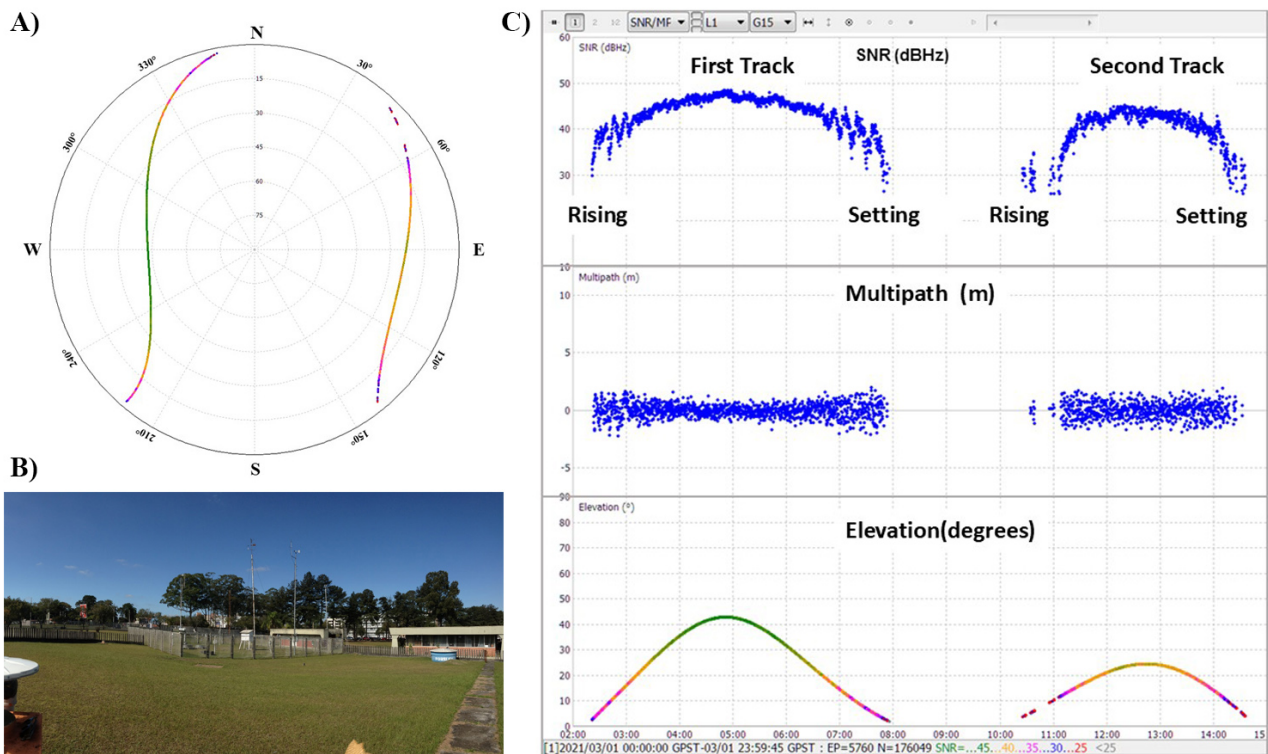


Figure 3 Skyplot, oscillations analysis, and obstructions of UFPR station: Skyplot of PRN15 GPS satellite - L1 signal, RTKlib software; B. Southeast View of the RBMC-UFPR station; C. Oscillation in RTKlib software.

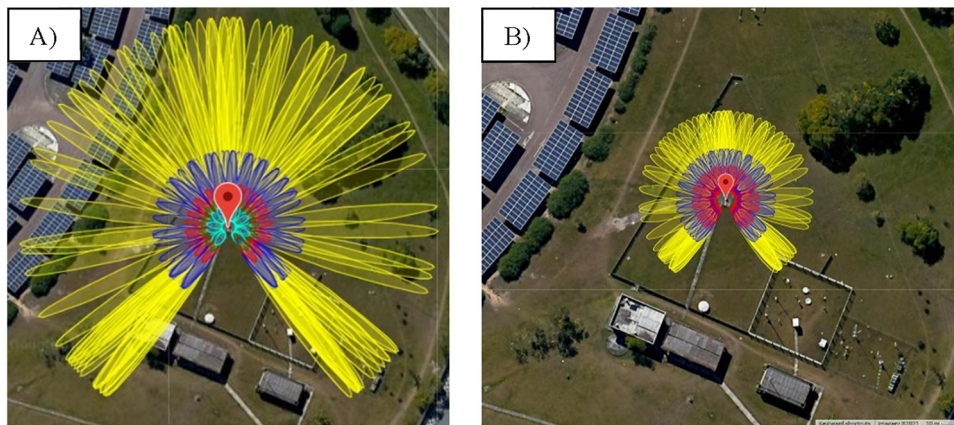


Figure 4 GNSS-IR footprint - GNSS-IR Reflection Zone Mapping: A. Elevation angles between 5° in yellow and 25° in cyan; B. Elevation angles between 10° (yellow) and 20° (red).

2.4 Obstruction Mapping

A topographic mapping of the obstructions surrounding the station was conducted to enhance the evaluation of the reflected signals through the SNR series. In this survey, the surrounding elements were categorized and mapped regarding azimuth and elevation, considering a horizontal plane common to the GNSS station. Figure 5A shows the obstruction map.

The main obstructions at this station are trees, indicated in green. There are several metal structures in the vicinity, many of which, in the southeastern portion of the area, correspond to the instruments of the meteorological station. Buildings and some concrete lighting poles are indicated in yellow. On average, these obstructions are at an elevation of 5°. The southern portion concentrates most of the buildings, which, in this case, do not significantly affect the oscillations due to the satellites' orbits. Furthermore, the topographic survey indicated that these buildings are below the antenna horizon.

It can be observed that the trees located to the south (on the right in Figure 3B) correspond to the most significant obstructions, with approximately 20 degrees from the antenna horizon. This leads to a greater restriction in terms of elevation angles in the surroundings. The metal structures of the meteorological instrumentation can also be seen. These obstructions may affect the reflected signals at low elevation angles; therefore, these conditions were taken into account in the processing configurations of the reflectometry algorithm.

Figure 5B shows a panoramic view of the northeastern portion of the UFPR station. The largest obstruction in this case is a tree in the center of the image, which has an elevation of approximately 7 degrees above

the antenna horizon. In Figure 5C, the western portion of the station can be seen. As can be observed, the Western area has significantly fewer obstructions. The height of the wall is below the GNSS antenna horizon. Furthermore, well-defined oscillations originating from this region were observed by analyzing the oscillations.

Based on the evaluation stages of the reflected signals, it was observed that the signals coming from satellites close to the horizon (low elevation angles) were being affected by the surrounding obstructions. The combination of this information, along with assessments made during the quality control of the processing, will enable the establishment of a mask that defines the appropriate GNSS-IR coverage area for the UFPR station.

2.5 Input Data

The input data for the reflectometry algorithm are SNR information recorded in GNSS tracking files in the standard observation RINEX format (.o), in version 3 or higher, as from this version the SNR observable is recorded separately for each combination of GNSS signals in terms of frequency and available code. Since January 1, 2020, IBGE has been providing 1-second tracking files in RINEX version 3 format.

The equipment that makes up the UFPR station is multi-GNSS. Thus, various signals are recorded, including legacy signals and modern signals such as L5, L2C, and L1C. The signals from the GPS (G) and GLONASS (R) systems were used in this research, totaling 24 signals, 12 for each system, indicated here according to the Rinex nomenclature standard: G - C1C, C2W, C2X, C5X, L1C, L2W, L2X, L5X, S1C, S2W, S2X, and S5X; R - C1C, C1P, C2C, C2P, L1C, L1P, L2C, L2P, S1C, S1P, S2C, S2P.

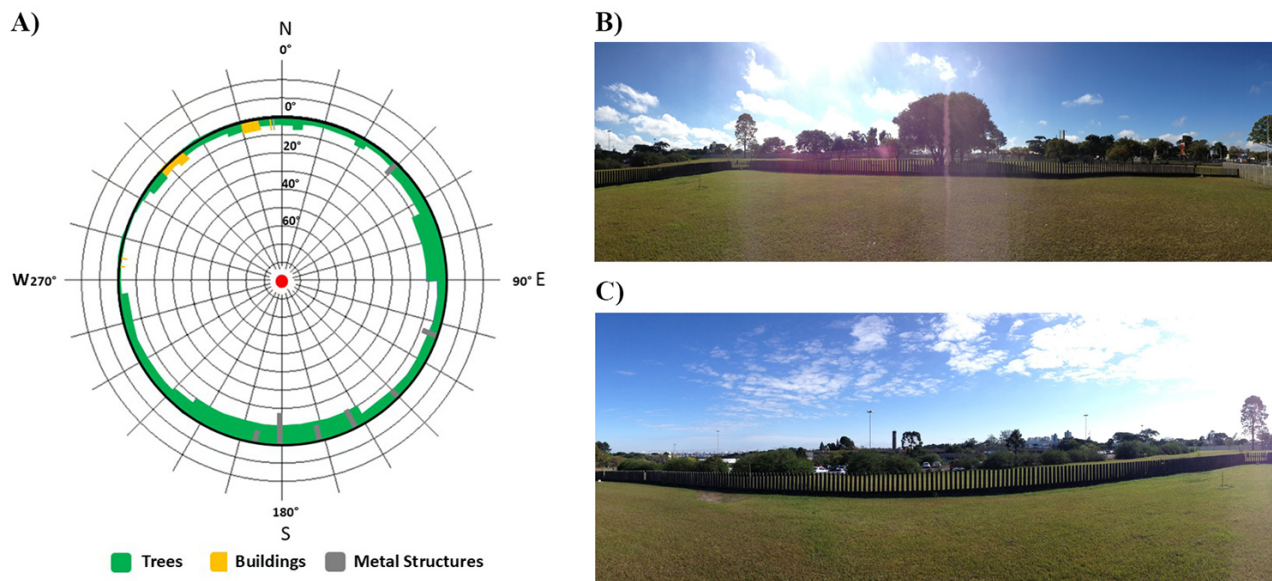


Figure 5 UFPR station surroundings: A. Obstruction mapping of RBMC-UFPR; B. UFPR station surroundings – Northeast direction; C. UFPR station surroundings – West direction.

Access to the RINEX files recorded by the UFPR station can be done through the IBGE website. The files are provided as 24-hour files for each station and are downloaded individually. Accessing the SNR observations from the RBMC for a given station and day requires: 1 – Download; 2 – Decompression of the file (.gz to .crx); 3 – Decompression of the compressed Rinex file (.crx to .rnx).

In this research, a period of 1 year (2022) was chosen for the investigations, based on several considerations: a complete year encompasses phenomena related to the different seasons, allowing for more consistent analyses of soil moisture patterns; since 2021, it has been possible to access GNSS data from the station with 1-second recording in RINEX format 3; from this period, there has been a gradual return to in-person activities in the context of the COVID-19 pandemic, so regular mowing activities around the station were already occurring normally; furthermore, as of November 27, 2022, the International GNSS Service (IGS) began adopting the IGS20 reference system, replacing IGS14 (IGS 2022; Altamini et al. 2021). This change requires an adaptation of the employed reflectometry algorithm.

In addition to the procedures for obtaining the RINEX files, the reflectometry algorithm requires that these files for the entire period of interest be in the same directory, properly organized with standard and sequential nomenclature, as per the example: ufpr0010.22o, where: “ufpr” is the station code; 001 is the day of the year (DoY - Day of Year), which can be checked using the GNSS Calendar tool (<https://www.gnsscalendar.com/>); “0” is the

8th digit, indicating the duration of the file is 24 hours, completing the standard RINEX nomenclature format with 8 digits. The extension “.22o” is the standard RINEX format to indicate the year corresponding to the file (2022) and the type of file, in this case, the observation file (.o). Other types of RINEX files, such as navigation files, e.g., .22n, are not used in reflectometry processing, as the algorithm automatically downloads the precise ephemerides during processing.

The exclusion of unnecessary observables for this processing is recommended. Thus, the carrier phase and pseudorange data also present in the observation files can be filtered out, as this information is not used in the reflectometry modeling. This filtering improves processing efficiency by reducing memory space.

Automating data processing is recommended when managing large volumes of information. In this context, an algorithm was developed in Python to download, convert, standardize, and filter GNSS data from the RBMC. Following IBGE guidelines, this algorithm was designed to prepare input data for any RBMC station by simply providing the station code and the period of interest. This algorithm makes it possible to automatically obtain RINEX files for the indicated period, for positioning or GNSS-IR. The algorithm is freely available on the GitHub platform (https://github.com/jorgeeuriques/gnssdata_rbmc). This algorithm includes the use of the tools crx2rnx (Hatanaka 2008), and gfrnx (Nischan 2016). Figure 6 illustrates the flowchart of the algorithm’s steps.

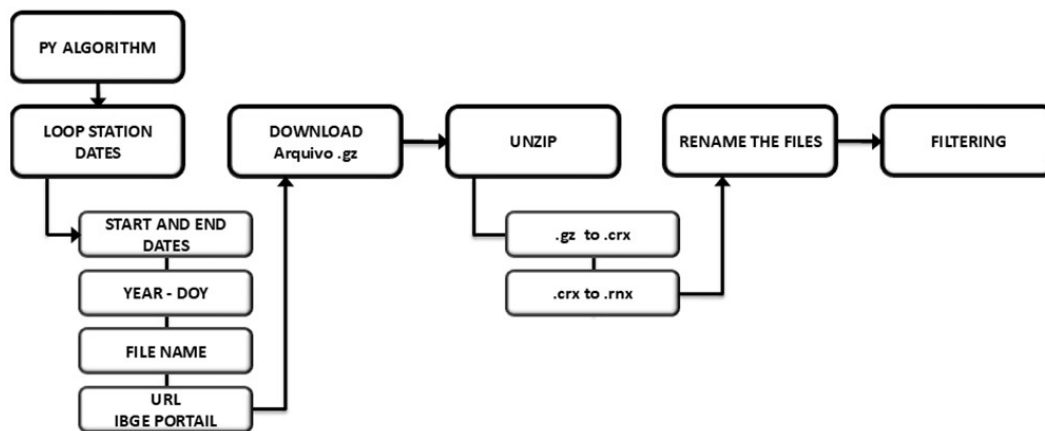


Figure 6 Python algorithm processing flow.

2.6 Reflectometric Algorithm

The employed reflectometric algorithm (Nievinski & Larson 2014a, 2014b, 2014c, 2014d) enables SNR modeling to facilitate GNSS-IR through two stages: inversion and post-processing. In the first stage, a combination of a physical model, related to the theoretical simulation of multipath, and an inverse model, through which parameters are estimated from GNSS observations measured in the field, is performed. The various configurations associated with these processes in the algorithm are crucial for obtaining consistent results.

Among these configurations are: satellite observation conditions; reference system; signal processing parameters; GNSS antenna electromagnetic responses; conditions related to reflections involving the reflecting surface; propagation medium; and parameter biases. Next, post-processing is carried out, which involves a quality control process and refinement of previously estimated parameters. In the case of processing to estimate soil moisture, values of the reflectometric phase are of particular interest (Euriques et al. 2021).

The algorithm developed is highly automated; however, during the post-processing stage, some interventions were necessary to define strategies that allowed the refinement of the results. These strategies included the introduction of constraints on certain correlated parameters, such as the antenna height and the reflectometric phase measurements, derived from the SNR series. Additionally, based on the results of this stage, new processing steps were conducted to adjust some configurations, such as applying azimuth and elevation angle masks to disregard directions affected by obstructions. These filters were applied by combining analyses performed with the RTKLIB software, the GNSS-IR Reflection Zone Mapping tool, and

the topographic mapping, along with the analysis of the reflectometric processing results. Elevation angles ranges were applied with three configurations: 0° to 30°; 5° to 30°; and 10° to 30°. The azimuth mask was gradually expanded, yielding better results when applied over the entire eastern portion of the station.

As a main result of these processes, reflectometric phase time series were obtained for each signal. All SNR signals, GPS and GLONASS, listed in section 2.4, were processed, with one processing run for each of these modulations. Other configurations were adjusted to present these results, which were refined by applying a moving average. A moving average is applied during the post-processing stage of the reflectometric algorithm to smooth short-term fluctuations and highlight trends in the phase time series. The moving average settings should be carefully evaluated to ensure an appropriate representation of the variables of interest.

Finally, after the reflectometric processing, an additional step was required to convert the reflectometric phase time series into soil moisture time series. This was accomplished through a calibration curve using theoretical coefficients indicated in the literature (Chew et al. 2014). The best results of this stage were achieved with the GS2X and RS2P signals. The time series obtained from these signals were compared with the precipitation events recorded by the INMET 807 station.

3 Results and Discussions

In Figures 7A and 7B the results of SNR modeling in the reflectometric processing can be observed. In red, the simulated SNR from the direct model is shown. In gray, the observed SNR adapted in the inversion module is displayed. In blue, the residual SNR represents the

difference between the simulated and observed SNR. These figures are generated for each modulation, satellite (PRN), and segment (ascending or descending arc of the satellite's position) within a given quadrant. Figure 7A corresponds to the SNR modeling of GPS satellite PRN08, DoY 001 (01/01/2022) at azimuth 220, considering the GS5X signal.

It can be indicated that the processing under these conditions was adequate, as the observed SNR series (dB) closely follows the simulated series, with residuals of ± 1 dB. In Figure 7B, the same configurations are applied, but for the GS2X signal. In this case, the magnitude of the residuals is around ± 2 dB. Although the GS2X signal shows a larger residual amplitude, it is worth noting that it was available on 24 satellites in 2022, while the GS5X signal was only available on 16 satellites. The L5 carrier presented a smaller magnitude of residuals; however, in addition to being associated only with GPS, it is not available for all satellites in this system. Thus, the SNR from the L2 carrier provided the best results in the processing stage for both evaluated systems, G and R. These findings are consistent with those reported in previous research, such as in Euriques (2019).

As with any modeling process, uncertainties are associated with the estimated parameters, which can be influenced, e.g. by the growth of vegetation around the antenna. Generally, it should be noted that the same satellite will have a series of figures associated with it, representing

the daily measurements by satellite, quadrant, year, and day. These figures were investigated as a complementary step to the prior evaluation of oscillations. The analysis of residuals also contributed to identifying azimuths that did not provide good reflections or were affected by obstructions.

The combination of these factors allowed for the establishment of masks in terms of azimuths or elevation angles in post-processing to filter the data. It was found that the best elevation angle mask used only the range between 10° and 30° above the antenna horizon. It should be noted that a very restrictive mask can affect the estimates, so it must be applied with caution. Additionally, the higher the elevation angle, the smaller the ellipses that compose the Fresnel surface, thus reducing the reflection area, which limits one of the advantages of GNSS-IR over other conventional soil moisture estimation techniques.

In Figures 8A and 8B, the biases and antenna height variation are presented for the different clusters defined by data grouping based on the satellite's azimuthal track. In Figure 8B, an azimuth mask was applied to filter the range defined by azimuths from 0 to 210° . In the case of a flat and horizontal surface, radial variability would be due only to estimation residuals. However, in practice, this variability occurs due to various factors, including instrumental noise, irregular surrounding topography, and genuine natural variability caused by vegetation growth around the station. These characteristics complicate the automation of this process.

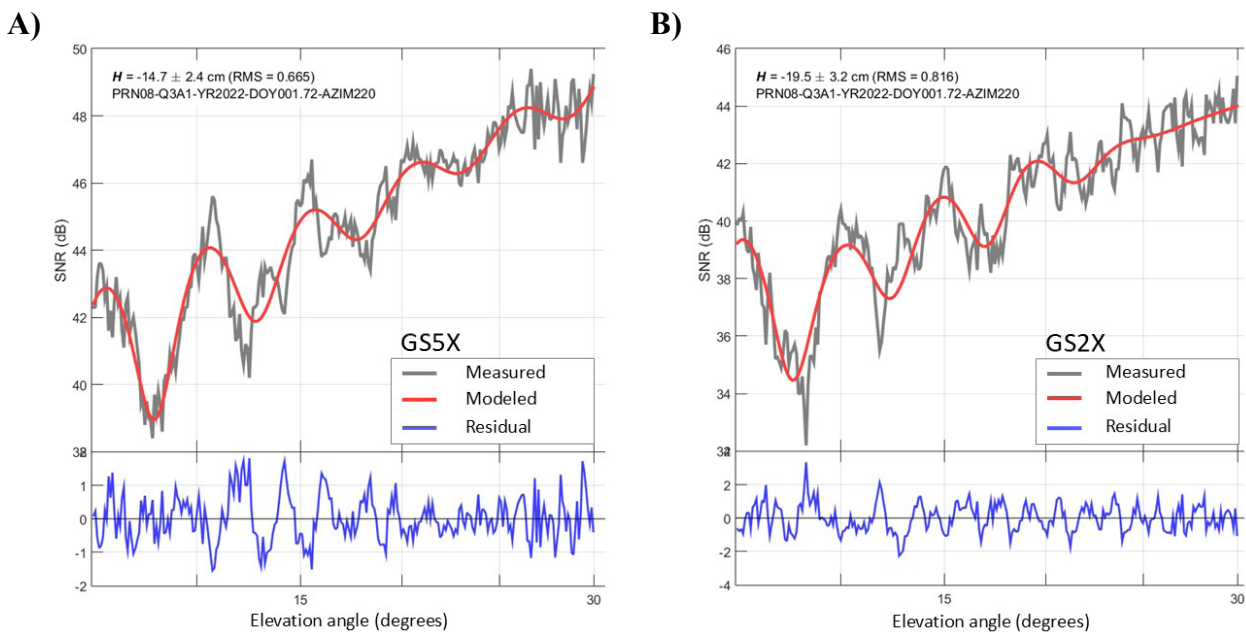


Figure 7 SNR plots by reflectometric algorithm: A. SNR plot by GS5X signal, Azimuth 220, DoY 001; B. SNR plot by GS2X signal, Azimuth 220, DoY 001.

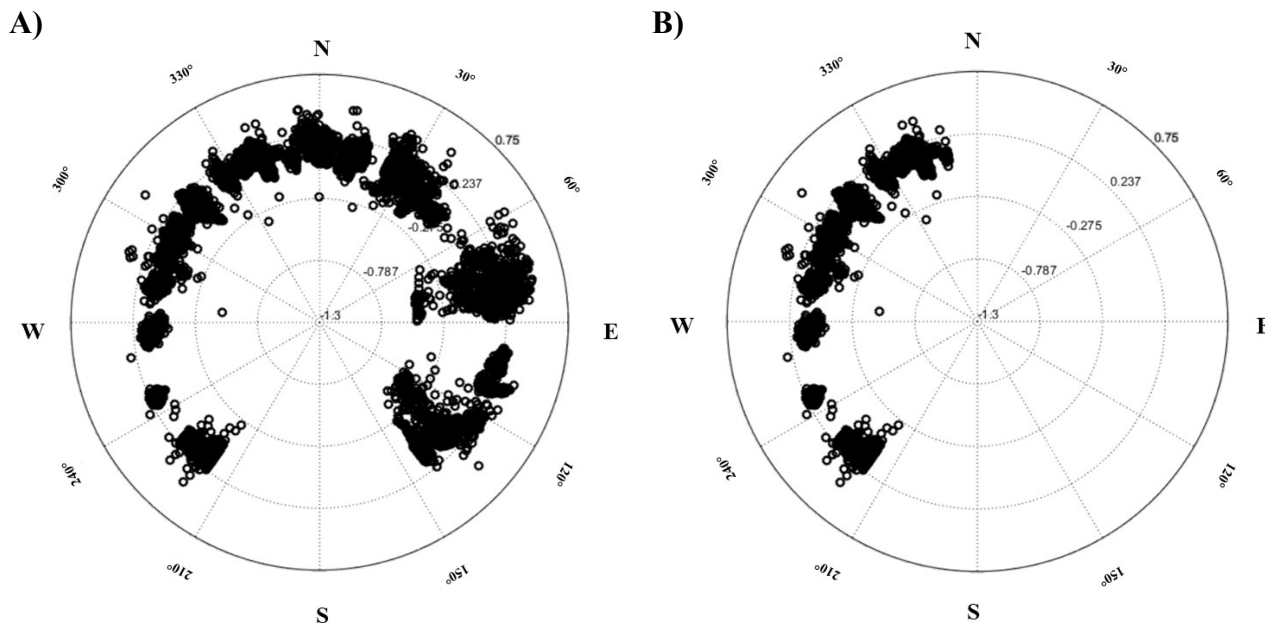


Figure 8 Antenna height biases as a function of azimuth: A. Before filtering; B. After filtering.

Regarding the moving average settings applied to the reflectometric phase time series, the hourly spacing was defined (1 phase value per hour), and different window widths were evaluated. Finally, from the reflectometric phase series, soil moisture is obtained through a calibration curve, which is applied after the processing by the reflectometric software. The theoretical coefficients of the calibration curve frequently reported in the literature the slope or angular coefficient (Chew et al. 2014) or reciprocally (Vey et al. 2016). This means that a change of 1° in phase corresponds to a change of $0.015 \text{ m}^3/\text{m}^3$ in the soil moisture content. These coefficient values were determined from physical simulations, considering the specific antenna models of the study receivers. The intercept or constant coefficient of the regression (b) is associated with the residual soil moisture, which represents the minimum soil moisture value, usually assumed to be (Vey et al. 2016). According to Chew et al. (2014), this coefficient can also be obtained by interpolation of soil texture maps. This minimum soil moisture value is associated with a minimum phase, which, in turn, depends on the antenna model used and can take an arbitrary value based on the characteristics of the considered station.

Figure 9 illustrates the reflectometric phase series (in degrees) throughout the epochs of the year 2022 (decimal year), obtained from the GS2X signal with a window width

of the moving average of 6h. It is observed that the series is interrupted around 2022.9. This happens because the period between 2022.9 and 2022.10 corresponds to the satellite orbit reference system change, officially adopted by the IGS, took place.

Figure 10 shows the soil moisture series derived from the reflectometric series presented in Figure 9. In this series, soil moisture ranges between 0 and $0.4 \text{ m}^3/\text{m}^3$. It is noted that the series is discontinued at epoch 2022.9, which coincides with the period when the reference system for satellite orbits was changed.

The precipitation events were plotted by downloading the data provided by INMET to compare them with the resulting soil moisture series. It was identified that the RS2P signal, specifically the precise signal of the L2 carrier wave from GLONASS, showed the best correspondence with the precipitation events when considering the same processing configurations. In the upper panel of Figure 11, the soil moisture series estimated from the RS2P signal is shown. It can be observed that, in this case, the moisture varies approximately between 0 and $0.35 \text{ m}^3/\text{m}^3$. For GLONASS, the series is normally represented throughout the entire year of 2022, even after the transition from IGB14 to IGS20 (2022.9). The precipitation graph (mm/day) for the year is presented in the lower panel.



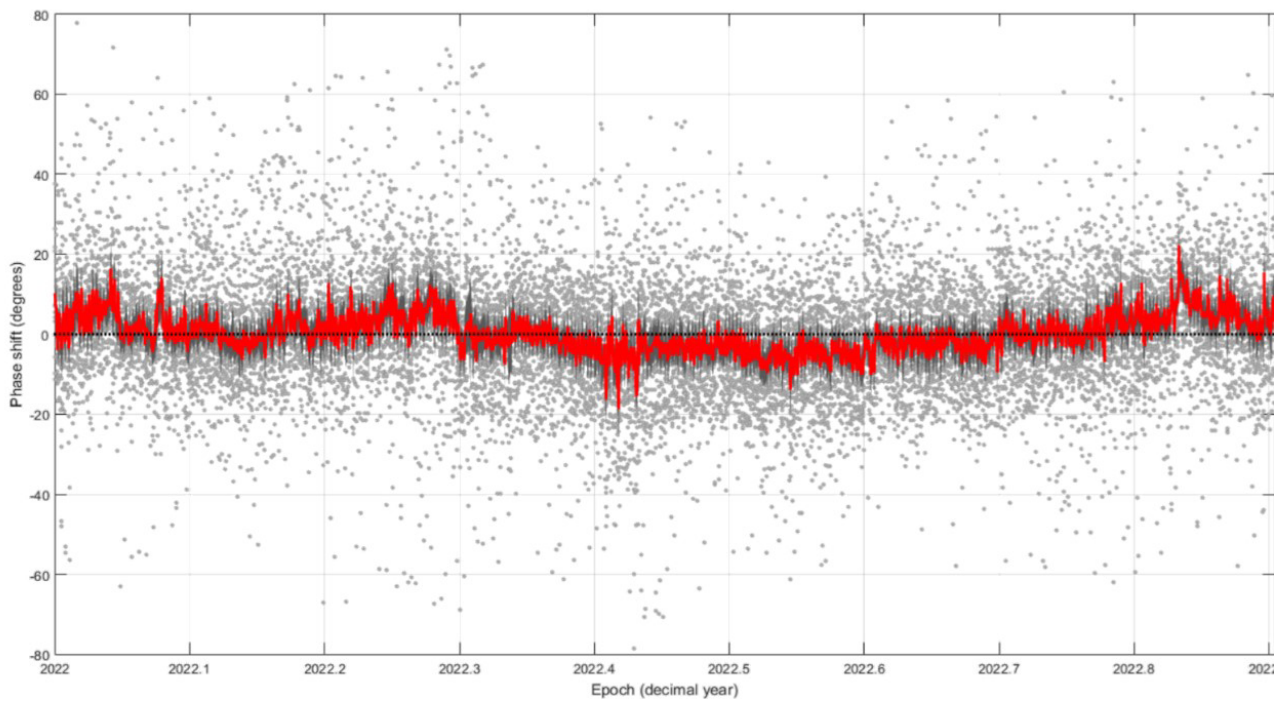


Figure 9 Reflectometric Phase – GS2X.

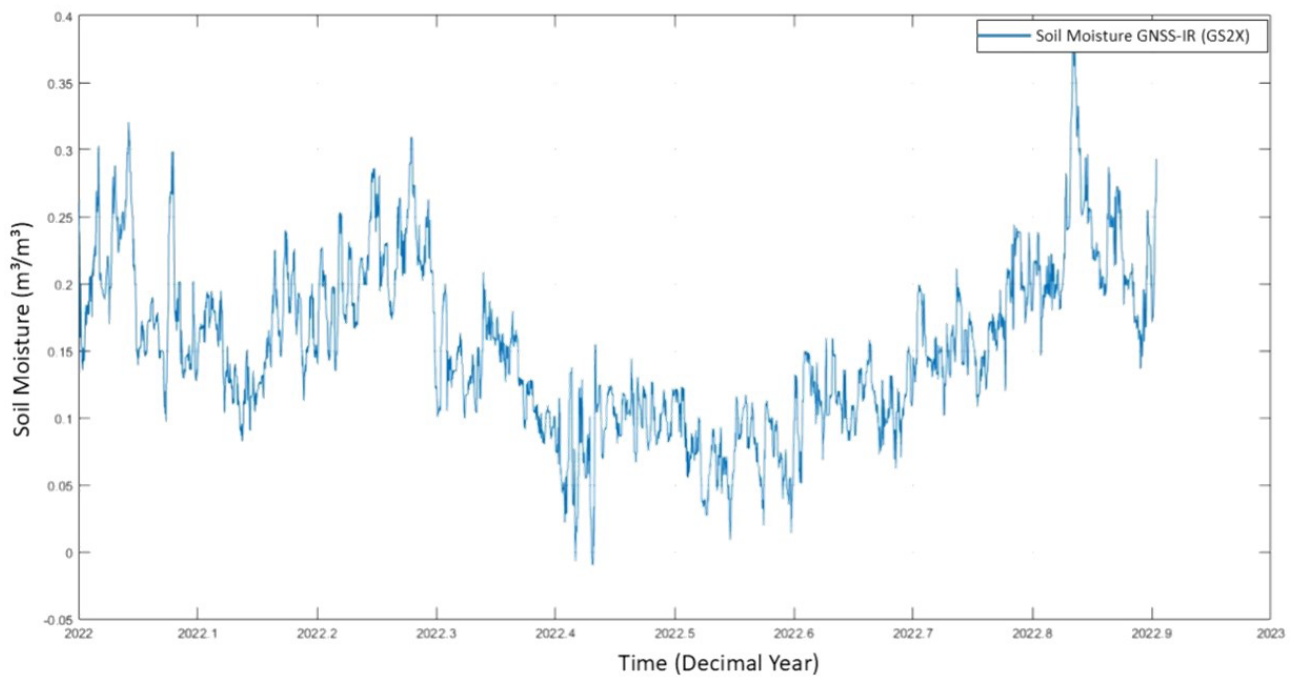


Figure 10 Soil Moisture time series: GNSS-IR– GS2X.



Soil moisture varies with depth and also horizontally due to several factors. In the more superficial layers, moisture variation is greater due to the direct effects of precipitation, evaporation, and runoff. The reference depth for soil moisture estimates using GNSS-IR is associated with more superficial layers, with depths of up to 5 cm, due to the penetration power of electromagnetic waves related to GNSS frequencies in the soil (Edokossi et al. 2020). Therefore, it is expected that soil moisture estimated by GNSS-IR will exhibit a highly variable behavior, as evidenced in Figure 10, where the moving average configurations resulted in less data smoothing compared to what is seen in Figure 11. When comparing with precipitation events, it is advisable to use more restrictive moving average settings to highlight more consistent phenomena, such as the direct contribution of precipitation to soil moisture.

Analyzing Figure 11, it is noticeable that the peaks in soil moisture occur simultaneously with precipitation events, as shown in situation 1 in the upper panel. In this regard, it is important to emphasize that the moving average settings, especially in terms of window width, should be carefully configured, as they can excessively smooth out isolated events.

It is observed that when the soil is relatively dry and precipitation events occur, moisture moves downward more slowly, initially remaining closer to the surface (scenario 2). When the soil is wetter and precipitation events occur, the opposite process happens: the surface soil loses moisture more quickly (scenario 3), remaining wetter at greater depths. From epoch 2022.7, after a period of relatively regular maximum precipitation peaks, and increasingly higher after 2022.8, a growing trend of increased soil moisture emerges (scenario 4).

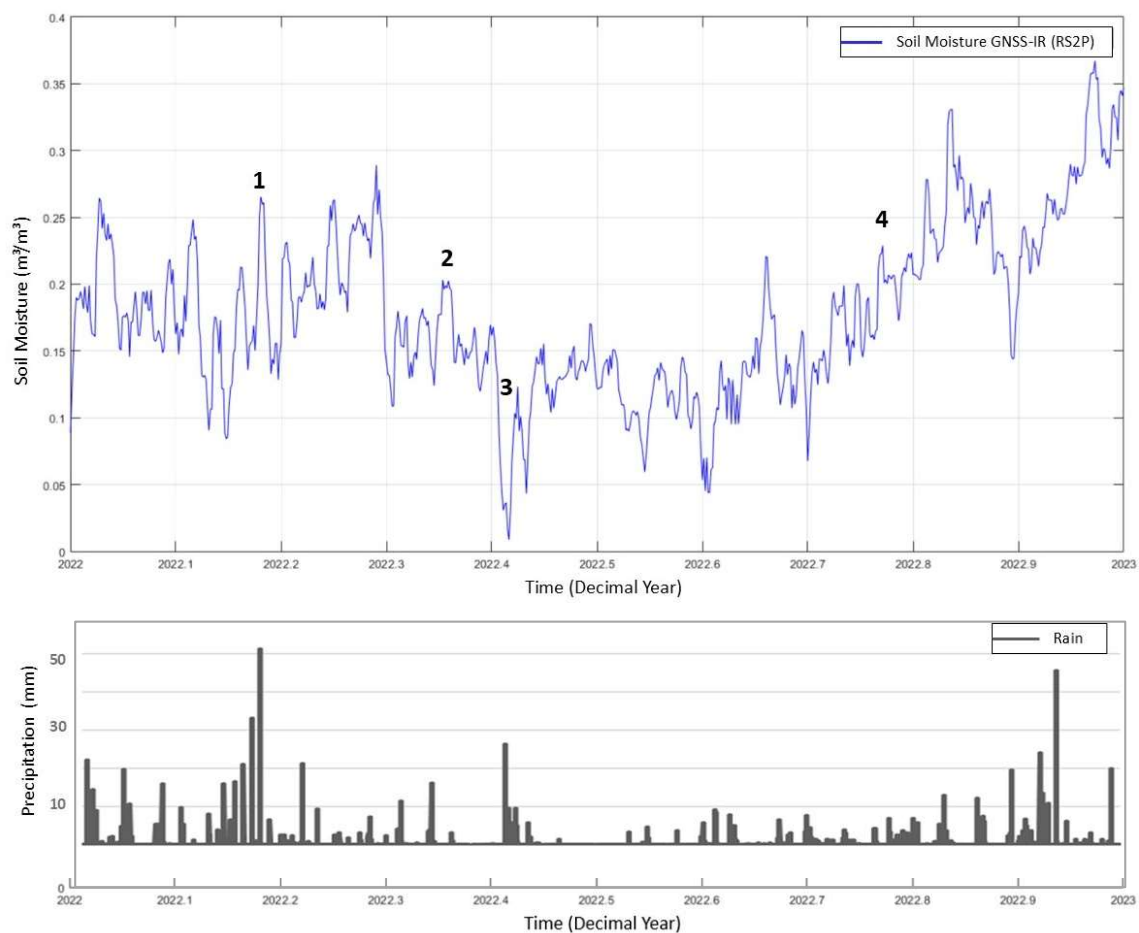


Figure 11 Soil Moisture time series x precipitation events.

4 Conclusion

Based on the presented results, it is possible to affirm that the continuously recorded data from the UFPR station of the RBMC was successfully used to estimate soil moisture around the station using the GNSS-IR technique. The results show correspondence with precipitation events recorded by a rain gauge from INMET located near the GNSS station.

Investigations were carried out to make a methodology for estimating soil moisture feasible for other RBMC stations that meet the requirements of the GNSS-IR technique. In this regard, the development of a Python algorithm for downloading, converting, standardizing, and filtering GNSS data, based on the data available on the IBGE portal, is highlighted. This algorithm is available on the GitHub platform. It can be used to automate the preparation of GNSS data from any RBMC station to GNSS-IR or positioning applications.

An evaluation of the configurations of the employed reflectometric algorithm was carried out, including elevation and azimuth masks defined by a combination of oscillation assessments using RTKLIB software and the GNSS-IR Reflection Zone Mapping tool, as well as a topographic survey.

Additionally, the results were evaluated based on different signals defined by the modulation/frequency combination of GPS and GLONASS. The best results are associated with the L2 carrier wave. Thus, it is considered that opportunistic soil moisture monitoring using GNSS-IR from RBMC stations can be carried out at a low cost, since no modifications to the existing equipment are necessary and the data is distributed free of charge by IBGE. The results can be made available to the public and may improve the modeling of various phenomena. In this way, they can contribute to national institutions such as the Brazilian Agricultural Research Corporation (In Portuguese, Empresa Brasileira de Pesquisa Agropecuária - EMBRAPA), the National Center for Monitoring and Early Warning of Natural Disasters (In Portuguese Centro Nacional de Monitoramento e Alerta de Desastres Naturais - CEMADEN), the National Water Agency (In Portuguese, Agência Nacional das Águas - ANA), and INPE.

In future works, it is recommended to validate the results using data from conventional soil moisture measurement sensors, such as TDR probes, as well as data obtained from satellite missions, which could contribute to direct analyses of soil moisture results.

5 Acknowledgments

The authors would like to thank colleagues Prof. Paulo Sergio de Oliveira Junior (UFPR), Allan Gomes

(IFSC), and Fabiano Freiman (UFBA) for their contributions to the work. The authors would like to thank CNPq (grant number 406486/2023-9) for its support in financing the project ‘Métodos geodésicos aplicados à estimação da umidade do solo e do total de água armazenada,’ in which this research is included. The work of J. F. Euriques was supported by the Brazilian Coordination of Superior Level Staff Improvement (CAPES) process N° 88882.382285/2019-01.

6 References

- Acharya, T.D. & Lee, D.H. 2019, ‘Remote sensing and geospatial technologies for sustainable development: A review of applications’, *Sensors and Materials*, vol. 31, n. 11, pp. 3931-45.
- Altamimi, Z., Rebischung, P.P., Métivier, L. & Collilieux, X. 2016, ‘ITRF2014: A new release of the International Terrestrial Reference Frame modeling nonlinear station motions’, *Journal of Geophysical Research: Solid Earth*, vol. 121, n. 8, pp. 6109-31.
- Altamimi, Z., Rebischung, P.P., Métivier, L. & Collilieux, X. 2021, ‘ITRF2020: An enhanced realization of the International Terrestrial Reference Frame’, *Journal of Geophysical Research: Solid Earth*, vol. 126, n. 10, e2020JB021490.
- Arroyo, A.A., Camps, A., Aguasca, A., Forte, G.F., Moneris, A., Rüdiger, C., Walker, J.P., Park, H., Pasucal, D. & Onrubia, R. 2014, ‘Dual-polarization GNSS-R interference pattern technique for soil moisture mapping’, *IEEE Journal of Selected Topics in Applied Earth Observations and Remote Sensing*, vol. 7, n. 5, pp. 1533-44.
- Awange, J.L. & Kyalo Kiema, J.B. 2013, *Environmental Geoinformatics*, Springer Berlin Heidelberg, Berlin.
- Babaeian, E., Sadeghi, M., Jones, S.B., Montzka, C., Vereecken, H. & Tuller, M. 2019, ‘Ground, Proximal, and Satellite Remote Sensing of Soil Moisture’, *Reviews of Geophysics*, vol. 57, n. 2, pp. 530-616.
- Chew, C.C., Small, E.E., Larson, K.M., Zavorotny, V.U. 2014, ‘Effects of near-surface soil moisture on GPS SNR data: Development of a retrieval algorithm for soil moisture’, *IEEE Transactions on Geoscience and Remote Sensing*, vol. 52, n. 1, pp. 537-43.
- Edokossi, K., Calabria, A., Jin, S. & Molina, I. 2020, ‘Gnss-reflectometry and remote sensing of soil moisture: A review of measurement techniques, methods, and applications’, *Remote Sensing*, vol. 12, n. 4.
- Entekhabi, D., Njoku, E.G., O’neill, P.E., Kellogg K.H., Crow, W., Edelstein, W.N., Entin, J., Goodman, S.D., Jackson, T.J., Johnson, J.T., Kimball, J.S., Piepmeier, J.R., Koste, R.D., Martin, N., Mcdonald, K., Moghaddam, M., Moran, S., Reichle, R., Shi, J., Spencer, M.W., Thurman, S., Tsang, L. & van Zyl, J. 2010, ‘The soil moisture active passive (SMAP) mission’, *Proceedings of the IEEE*, vol. 98, n. 5, pp. 704-16.
- Euriques, J.F. 2019, ‘Determinação da umidade do solo por meio da técnica de Refletometria GNSS – Primeiros resultados no Brasil’, Master’s thesis, Universidade Federal do Paraná.

- Euriques, J.F., Krueger, C.P., Machado, W.C., Sapucci, L.F. & Geremia-Nievinski, F. 2021, 'Soil Moisture Estimation with GNSS Reflectometry: A Conceptual Review', *Revista Brasileira de Cartografia*, vol. 73, n. 2, pp. 413-34.
- Georgiadou, P.Y. & Kleusberg, A. 1988, 'On Carrier Signal Multipath Effects in Relative GPS Positioning', *Map Collector*, vol. 13, pp. 172-79.
- Geremia-Nievinski, F. & Hobiger, T. 2019, 'Site guidelines for multi-purpose GNSS reflectometry stations', *Zenodo*.
- Hatanaka, Y. 2008, 'A Compression Format and Tools for GNSS Observation Data', *Bulletin of the Geospatial Information Authority of Japan*, vol. 55, pp. 21-30.
- Hillel, D. 1998, *Environmental Soil Physics*, Academic Press, San Diego.
- Instituto Brasileiro de Geografia e Estatística – IBGE & RBMC – Rede Brasileira de Monitoramento Contínuo dos Sistemas GNSS 2024, 'Relatório de Informação de Estação UFPR – Curitiba', viewed 10 June 2024, <https://geofp.ibge.gov.br/informacoes_sobre_posicionamento_geodesico/rbmc/relatorio/Descritivo_UFPR.pdf>.
- International GNSS Service – IGS 2022, 'Adoption of IGS20 Reference Frame', viewed 10 June 2024, <<https://igs.org>>.
- Instituto Nacional de Meteorologia – INMET 2023, 'Climatologia: Dados e informações climáticas', viewed 10 June 2024, <<http://www.inmet.gov.br>>.
- Jin, S., Cardellach, E. & Xie, F. 2014, *Remote Sensing and Digital Image Processing: Theory, Methods and Applications*, Springer International Publishing, Switzerland.
- Larson, K.M. 2024, 'Gnssrefl: An open source software package in python for GNSS interferometric reflectometry applications', *GPS Solut*, vol. 28, no. 165.
- Larson, K.M., Braun, J.J., Small, E.E., Zavorotny, V.U., Senior Member, IEEE, Gutmann, E.D. & Bilich, A.I. 2010, 'GPS Multipath and Its Relation to Near-Surface Soil Moisture Content', *IEEE Journal of Selected Topics in Applied Earth Observations and Remote Sensing*, vol. 3, no. 1, pp. 91-9.
- Larson, K.M. & Nievinski, F.G. 2013, 'GPS snow sensing: Results from the EarthScope Plate Boundary Observatory', *GPS Solutions*, vol. 17, no. 1, pp. 41-52.
- Larson, K. M., Small, E. E., Gutmann, E., Bilich, A., Axelrad, P. & Braun, J.J. 2008a, 'Using GPS multipath to measure soil moisture fluctuations: Initial results', *GPS Solutions*, vol. 12, no. 3, pp. 173-77.
- Larson, K.M., Small, E.E., Gutmann, E.D., Bilich, A., Braun, J.J. & Zavorotny, V.U. 2008b, 'Use of GPS receivers as a soil moisture network for water cycle studies', *Geophysical Research Letters*, vol. 35, no. 24.
- Leick, A. 1995, *GPS Satellite Surveying*, 2nd edn, John Wiley & Sons, New York.
- Li, Y., Yu, K., Li, J., Jin, T., Chang, X., Zhang, Q. & Yang, S. 2022, 'Measuring soil moisture with refracted GPS signals', *IEEE Geosci Remote Sens Lett*, vol. 19, pp.1-5.
- Martín, A., Ibáñez, S., Baixauli, C., Blanc, S. & Julián, A.B.A. 2020, 'Multi-constellation GNSS interferometric reflectometry with mass-market sensors as a solution for soil moisture monitoring', vol. 24, no. 7, pp. 3573-82.
- Nischan, T. 2016, *GFZRN X - RINEX GNSS Data Conversion and Manipulation Toolbox*, viewed 10 June 2024, <<https://doi.org/10.5880/GFZ.1.1.2016.002>>.
- Nievinski, F.G. & Larson, K.M. 2014a, 'Forward modeling of GPS multipath for near-surface reflectometry and positioning applications', *GPS Solutions*, vol. 18, no. 2, pp. 309-22.
- Nievinski, F.G. & Larson, K.M. 2014b, 'An open source GPS multipath simulator in Matlab/Octave', *GPS Solutions*, vol. 18, no. 3, pp. 473-81.
- Nievinski, F.G. & Larson, K.M. 2014c, 'Inverse modeling of GPS multipath for snow depth estimation - Part I: Formulation and simulations', *IEEE Transactions on Geoscience and Remote Sensing*, vol. 52, no. 10, pp. 6555-63.
- Nievinski, F.G. & Larson, K.M. 2014d, 'Inverse modeling of GPS multipath for snow depth estimation - Part II: Application and validation', *IEEE Transactions on Geoscience and Remote Sensing*, vol. 52, no. 10, pp. 6564-73.
- Nievinski, F.G., Silva, M.F.E., Boniface, K. & Monico, J.F.G. 2016, 'GPS Diffractive Reflectometry: Footprint of a Coherent Radio Reflection Inferred from the Sensitivity Kernel of Multipath SNR', *IEEE Journal of Selected Topics in Applied Earth Observations and Remote Sensing*, vol. 9, no. 10, pp. 4884-91.
- Ochsner, T.E., Cosh, M.H., Cuenca, R.H., Dorigo, W.A., Draper, C.S., Hagimoto, Y., Kerr, T.H., Larson, K.M., Njoku, E.G., Small, E.E. & Zreda, M. 2013, 'State of the Art in Large-Scale Soil Moisture Monitoring', *Soil Science Society of America Journal*, vol. 77, no. 6, pp. 1888-923.
- Paganini, M., Petiteville, I., Ward, S., Dyke, G., Steventon, M. & Harry, J. 2018, *Satellite Earth Observations in support of the Sustainable Development Goals*, European Space Agency (ESA), Paris.
- Plag, H.P. & Pearlman, M. (ed.). 2009, *Global Geodetic Observing System*, Springer, Switzerland.
- Robinson, D.A., Campbell, C.S., Hopmans, J.W., Hornbuckle, B.K., Jones, S.B., Knight, R., Ogden, F., Selker, J. & Wendroth, O. 2008, 'Soil Moisture Measurement for Ecological and Hydrological Watershed-Scale Observatories: A Review', *Vadose Zone Journal*, vol. 7, no. 1, pp. 358-89.
- Rodriguez-Alvarez, N., Bosch-Lluis, X., Camps, A., Vall-llossera M., Valencia, E., Marchn-Hernandes, J.F. & Ramoz-Perrez, I. 2009, 'Soil moisture retrieval using GNSS-R techniques: Experimental results over a bare soil field', *IEEE Transactions on Geoscience and Remote Sensing*, vol. 47, no. 11, pp. 3616-24.
- Roussel, N., Frappart, F., Ramillien, G., Darrozes, J., Baup, F., Lestarquit, L. & Ha, M.C. 2016, 'Detection of Soil Moisture Variations Using GPS and GLONASS SNR Data for Elevation Angles Ranging from 2° to 70°', *IEEE Journal of Selected Topics in Applied Earth Observations and Remote Sensing*, vol. 9, no. 10, pp. 4781-94.
- Roussel, N., Ramillien, G., Frappart, F., Darrozes, J., Gay, A., Biancale, R., Striebig, N., Hanquez, V., Bertin, X. & Allain, D. 2015, 'Sea level monitoring and sea state estimate using a single geodetic receiver', *Remote Sensing of Environment*, vol. 171, pp. 261-77.
- Seeber, G. 2003, *Satellite Geodesy: Foundations, Methods, and Applications*, 2nd edn, Walter de Gruyter, New York.
- Seneviratne, S.I., Corti, T., Davin, E.L., Hirschi, M., Jaeger, E.B., Lehner, I., Orlowsky, B. & Teuling, A. 2010, 'Investigating soil moisture-climate interactions in a changing climate: A review', *Earth-Science Reviews*, vol. 99, no. 3-4, pp. 125-61.

- Simon, P., Hollingsworth, A., Carli, B., Källén, E., Rott, H., Partington, K.C., Moreno, J., Schaeppman, M., Mauser, W., Flemming, N., Visbeck, M., Vermeersen, B.L.A., Friis-Christensen, F., Johannessen, J.A., Kelder, H., Kosuth, P., Nadia, P., Quegan, S. & Sobrinho, J. 2006, *The Changing Earth : New scientific challenges for ESA's Living Planet Programme*, ESA Publications Division, Paris.
- Tabibi, S., Nievinski, F.G. & Van Dam, T. 2017, 'Statistical Comparison and Combination of GPS, GLONASS, and Multi-GNSS Multipath Reflectometry Applied to Snow Depth Retrieval', *IEEE Transactions on Geoscience and Remote Sensing*, vol. 55, no. 7, pp. 3773-85.
- Tabibi, S., Nievinski, F.G., Van Dam, T. & Monico, J.F.G. 2015, 'Assessment of modernized GPS L5 SNR for ground-based multipath reflectometry applications', *Advances in Space Research*, vol. 55, no. 4, pp. 1104-16.
- Teunissen, P.J.G. & Montenbruck, O. (ed.). 2017, *Springer Handbook of Global Navigation Satellite Systems*, Springer International Publishing, Switzerland.
- Vey, S., Güntner, A., Wickert, J., Blume, T. & Ramatschi, M. 2016, 'Long-term soil moisture dynamics derived from GNSS interferometric reflectometry: a case study for Sutherland, South Africa', *GPS Solutions*, vol. 20, no. 4, pp. 641-54.
- Wang, Q., Zheng, Y., Xu, S., Zhou, G. & Yu, J. 2022, 'In situ mesoscale soil moisture content monitoring based on global navigation satellite system interferometric reflectometry and ensemble modeling', *Journal of Applied Remote Sensing*, vol.16, no. 02, pp.1-17.
- Wei, H., Yang, X., Pan, Y. & Shen, F. 2023, 'GNSS-IR Soil Moisture Inversion Derived from Multi-GNSS and Multi-Frequency Data Accounting for Vegetation Effects', *Remote Sensing*, vol.15 no. 22.
- Wu, X., Ma, W., Xia, J., Bai, W., Jin, S. & Calabria, A. 2021, 'Spaceborne GNSS-R soil moisture retrieval: Status, development opportunities, and challenges', *Remote Sensing*, vol. 13, no. 1, pp. 1-24.
- Yan, S. H., Zhang, N., Chen, N.C. & Gong, J.Y. 2018, 'Feasibility of using signal strength indicator data to estimate soil moisture based on GNSS interference signal analysis', *Remote Sensing Letters*, vol. 9, no. 1, pp. 61-70.
- Yang, T., Wan, W., Chen, X., Chu, T., Qiao, Z., Liang, H., Wei, J., Wang, G. & Hong, Y. 2019, 'Land surface characterization using BeiDou signal-to-noise ratio observations', *GPS Solutions*, vol. 23, no. 2, pp. 1-12.
- Yang, T., Wan, W., Chen, X., Chu, T. & Hong, Y. 2017, 'Using BDS SNR observations to measure near-surface soil moisture fluctuations: Results from low vegetated surface', *IEEE Geoscience and Remote Sensing Letters*, vol. 14, no. 8, pp. 1308-12.
- Zavorotny, V.U., Gleason, S., Cardellach, E. & Camps, A. 2014, 'Tutorial on remote sensing using GNSS bistatic radar of opportunity', *IEEE Geoscience and Remote Sensing Magazine*, vol. 2, no. 4, pp. 8-45.
- Zavorotny, V.U. & Voronovich, A.G. 2000, 'Scattering of GPS signals from the ocean with wind remote sensing application', *IEEE Transactions on Geoscience and Remote Sensing*, vol. 38, no. 2, pp. 951-64.
- Zhang, S., Roussel, N., Boniface, K., Ha, M.C., Frapart, F., Darrozes, J., Baup, F. & Calvet, J.-C. 2017, 'Use of reflected GNSS SNR data to retrieve either soil moisture or vegetation height from a wheat crop', *Hydrology and Earth System Sciences*, vol. 21, no. 9, pp. 4767-84.
- Zhang, X., Nie, S., Zhang, C., Zhang, J. & Cai, H. 2021, 'Soil moisture estimation based on triple-frequency multipath error', *International Journal of Remote Sensing*, vol. 42, no. 15, pp. 5953-68.

Author contributions

Jorge Felipe Euriques: conceptualization; formal analysis; methodology; algorithm development; validation; writing-original draft; writing – review and editing; visualization. **Luis Augusto Koenig Veiga:** supervision. **Wagner Carrupt Machado:** conceptualization. **Claudia Pereira Krueger:** conceptualization. **Felipe Geremia-Nievinski:** conceptualization; methodology; and general supervision.

Conflict of interest

The authors declare no conflict of interest.

Data availability statement

The GNSS data used for the modeling were obtained from the IBGE portal (<https://www.ibge.gov.br>). The models used in this study were previously published in Nievinski and Larson (2014a, 2014b, 2014c, 2014d). Additional scripts, including those developed specifically for this study, will be available on GitHub (https://github.com/jorgeeuriques/gnssdata_rbmc), and further details can be provided upon request.

How to cite:

Euriques, J.F.E., Veiga, L.A.K., Machado, W.C., Krueger, C.P. & Nievinski, F.G. 2025, 'Soil Moisture Estimation by GNSS-IR from Active Stations: Case Study – RBMC/IBGE, UFPR Station', *Anuário do Instituto de Geociências*, vol. 48, e65911, DOI: 10.11137/1982-3908_2025_48_65911.

